

Structure of $EuCrO_4$ and Its Electronic and Magnetic Properties

Hidetaka Konno,* Yoshitaka Aoki, Zoltán Klencsár,† Attila Vértes,† Makoto Wakeshima,†† Keitaro Tezuka,†† and Yukio Hinatsu††

Graduate School of Engineering, Hokkaido University, Sapporo 060-8628

†Hungarian Academy of Sciences at Eötvös Loránd University, 1117 Budapest, Hungary

††Graduate School of Science, Hokkaido University, Sapporo 060-0810

(Received June 20, 2001)

Single phase zircon type $EuCrO_4$ (S.G. $I4_1/amd$) was synthesized and the structure including atomic positions was precisely determined by X-ray Rietveld refinement. The electronic and magnetic properties of the compound were studied based on the electric conductivity, Seebeck coefficient, Raman spectroscopy, Mössbauer spectroscopy, magnetic susceptibility, and specific heat. The CrO_4^{3-} tetrahedra in $EuCrO_4$ were slightly elongated compared with that in $NdCrO_4$, which caused splitting of the degenerated vibration modes of CrO_4^{3-}, ν_2 and ν_3, in the Raman spectra. The ^{151}Eu Mössbauer spectra showed not a trace of the Eu(II) species in the compounds measured in the present work. The Debye temperature, Θ_D, estimated from Mössbauer spectra suggested that the vibrational state of Eu(III) in $EuCrO_4$ was similar to that in the perovskite-type $EuCrO_3$. However, the isomer shift of Mössbauer spectra revealed that the electron density of the 6s orbital of Eu(III) in $EuCrO_4$ was very low and almost the same as that in the zircon type $EuVO_4$, that is, Eu(III) in these compounds has highly ionic character, whereas the electron density of the 6s orbital of Eu(III) in $EuCrO_3$ was higher and nearly the same as that in Eu_2O_3. $EuCrO_4$ was found to be an *n*-type semiconductor similar to $NdCrO_4$, while zircon type $REMO_4$ (RE: rare earth metal(III); M: V, P, As, etc.) are insulators. Magnetic susceptibility and specific heat measurements showed that antiferromagnetic transitions took place at around 15 K and was solely due to Cr(V) from the magnetic entropy value of 5.54 J mol^{-1} K^{-1}.

Rare earth metal(III) chromates(V), $RECrO_4$ (RE: rare earth metal(III)), are stable in an ambient atmosphere, and studies have been concentrated on their complex magnetic behavior due to the interaction between two kinds of magnetic ions, RE(III) and Cr(V).[1–5] In previous papers,[6,7] we have reported that $LaCrO_4$ and $Nd_{1-x}Ca_xCrO_4$ (x = 0–0.2) can be synthesized as a single phase by pyrolysis of the precursors prepared from stoichiometrically mixed solutions of RE(III), Ca(II) and Cr(VI), and have determined the detailed structure by X-ray Rietveld refinement and Raman spectroscopy. A series of compounds containing Nd(III) and Ca(II) are mixed valence ones of Cr(V) and Cr(VI).[7] By measurements of the electric conductivity, Seebeck coefficient and magnetic susceptibility, and from ab initio molecular orbital (MO) calculations, these compounds were found to be unique *n*-type semiconductors having a conduction band of antibonding $p\sigma^*$ states (O 2p origin)[8] due to the intermixing of the ligand-to-metal charge-transfer (LMCT) state.[9,10] This is a new finding, since normally monazite- and zircon types of $RE(MO_4)$ (M = P, V, As, and so on) are insulators. In the course of the studies described above, the structure and properties of CrO_4^{3-} tetrahedra were the subjects of general interest to us, since appropriate techniques to characterize the counter cation, RE(III), were not at hand, except for X ray diffraction (XRD) and X ray photoelectron spectroscopy (XPS). The information by XPS is confined to the surface, and the spectra of RE(III) are so complicated that the chemical states cannot be distinguished well. In addition, the reference data of XPS for the elements of atomic number 60–71 (Nd–Lu) are not sufficient.

We have started to synthesize compounds of atomic number 63–71 and yttrium.[11] Among them, europium is one of the most suitable nuclei for Mössbauer spectroscopy. In the present work, the detailed structure of $EuCrO_4$ including the vibrational structure and electronic configurations were investigated by X-ray Rietveld refinement, Raman spectroscopy, and Mössbauer spectroscopy, and the electric and magnetic properties were measured.

Experimental

The $EuCrO_4$ was synthesized by pyrolysis of the precursor in O_2. The precursor was prepared by vacuum drying of an equimolar solution of $Eu(CH_3COO)_3{\cdot}4H_2O$ and CrO_3 at 70 °C, followed by preheating at 400 °C in air. The details of the procedure are similar to those reported elsewhere.[6,7] The pyrolysis conditions of the precursor to form single phase $EuCrO_4$ were investigated by TG-DTA and XRD. The chemical composition of $EuCrO_4$ prepared as a single phase was determined by titration in the same manner as reported previously.[6]

X-ray diffraction patterns were measured by a JEOL 3500 diffractometer with a monochromator under the following conditions: Cu $K\alpha$, 30 kV, 300 mA; scanning step, 0.02 deg (2θ); counting time, 7–12 s $step^{-1}$. Structure refinement by the Rietveld method was carried out using the RIETAN program. Raman spectroscopic measurements were carried out by a triple-type monochromator (JASCO NRS-2000) under the irradiation of an argon

ion laser (514.2 nm) of 50 mW. The details of these measurements and analysis are the same with those reported previously.[6,7]

The ^{151}Eu Mössbauer spectra of $EuCrO_4$ were recorded in standard transmission geometry using a $^{151}SmF_3$ Mössbauer source with 9×10^9 Bq activity. For comparison, measurements of $EuCrO_3$ and $EuVO_4$, both synthesized in a usual manner, were carried out. The analysis of the Mössbauer spectra was performed by the MossWinn program[12] by assuming a pure quadrupole interaction between the ^{151}Eu nucleus and the neighboring electric charges. The spectra were analyzed by the least-squares fitting of Lorentzians using the full Hamiltonian of the excited $I_e = 7/2$ and ground $I_g = 5/2$ spin states. The quadrupole moments of the excited and the ground state were fixed to $Q_e = 1.5 \times 10^{-28}$ m^2 and $Q_g = 1.14 \times 10^{-28}$ m^2, respectively.[13] The ^{151}Eu isomer shifts are given relative to EuF_3. The spectra of $EuCrO_4$ and $EuCrO_3$ were measured at different temperatures between 15 K and room temperature, while that of $EuVO_4$ was measured only at room temperature.

The electric conductivity was measured in a dry oxygen atmosphere by the dc two-probe method using disk-shape samples of about 12 mm in diameter and 4 mm in thickness, which were prepared by the CIP method at 100 MPa and annealed at 813 K for 20 h in O_2. Both sides of the disks were coated with gold by physical vapor deposition and fine gold wires were connected to the disks with gold paste. A sample set in an alumina boat was placed on a Pt/Pt-13Rh thermocouple in an electric furnace. Ten data were accumulated with different applied currents at each temperature during heating and cooling cycles. The Seebeck coefficient was measured with rod-shape samples of about 2 mm in diameter and 16–20 mm long, prepared by the same method described above. Gold foils were attached to both ends and Pt/Pt-13Rh thermocouples were wound at the both ends. The sample was placed vertically in the lower part of a vertical furnace where the temperature gradient was less than 10 K cm^{-1}. Before any measurements of the Seebeck coefficient, more than one hour was allowed to pass after the temperatures at both contact points reached constant. The density of the sample was about 70% of the theoretical value because this compound cannot be sintered at temperatures below 1000 K, above which it decomposes to other compounds: single crystals are still not available. Regardless of the density, no differences in the properties were observed between samples prepared by different runs.

The temperature dependence of the magnetic susceptibility was measured at 0.1 T by a Quantum Design SQUID magnetometer after zero field cooling. The sample was set in a poly-chlorotrifluoroethylene container, and the signal from an empty container was subtracted from the experimental data.

The specific heat was measured by a relaxation technique using a Quantum Design PPMS system in the temperature range of 1.8–300 K. The sample pellet was mounted on a thin alumina plate with apiezon for better thermal contact.

Results and Discussion

A. Structure of $EuCrO_4$. Single phase and stoichiometric $EuCrO_4$ was obtained by pyrolysis of the precursor at 863 K for 3 h in O_2. For XRD and all other measurements to characterize $EuCrO_4$, samples were annealed at 813 K for 20 h in O_2. As already reported,[4,5,14] $EuCrO_4$ had zircon type structure similar to that of $NdCrO_4$ (S.G. $I4_1/amd$).[5,6] The XRD pattern and results of Rietveld refinement are shown in Fig. 1, where the calculated values are plotted by dots; the agreement is so excellent as shown by the difference curve that they are not distinguishable. The *d*-spacing, relative intensity and *hkl* index are summarized in Table 1 and crystallographic data together with reliability factors in Table 2. The Rietveld refinement was carried out with 132 peaks but the data for $2\theta > 90°$ are omitted in Table 1 due to the limitation of space. In the refinement, $EuVO_4$ was used as a starting model for the initial atomic position and thermal parameters,[15] and isotropic thermal parameters *B* were employed. As shown in Table 2, the reliability factors, R_{wp}, R_p, R_F and R_{exp}, are sufficiently small and *G* of *F* factor (goodness of fitting indicator R_{wp}/R_{exp}) which represents the quality of the refined structure is less than the required limit of

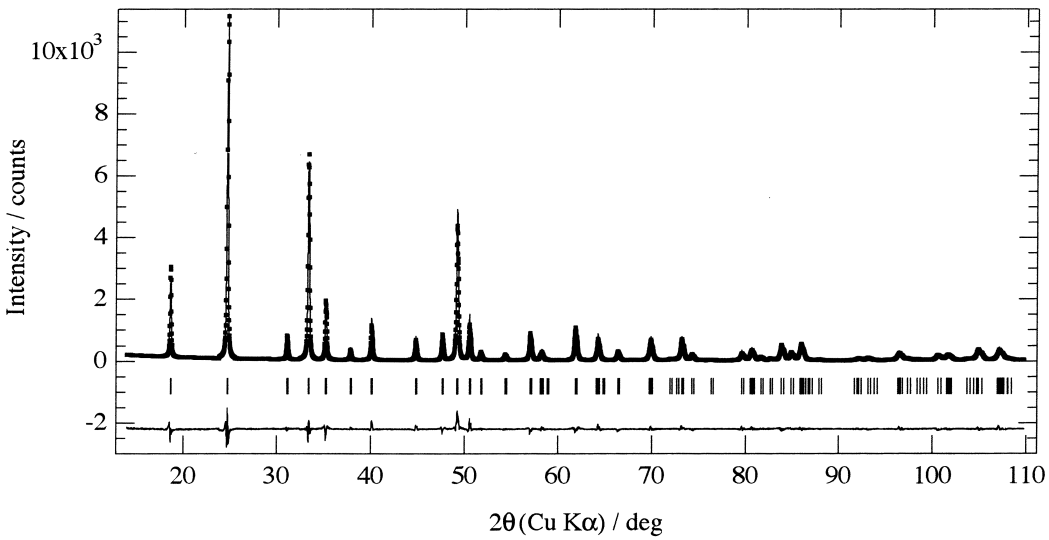

Fig. 1. The Power X-ray diffraction pattern and Rietveld refinement profile for $EuCrO_4$. The full line and dots show observed and calculated patterns, respectively. Tick marks indicate the positions of allowed Bragg reflection. The difference between the observed and calculated values is located at the bottom.

Table 1. The Observed and Calculated *d*-Spacing, Relative Intensity and *hkl* Indexing of XRD Powder Patterns for $EuCrO_4$. Data for $2\theta > 90°$ Were Cut Due to the Limitation of Space

hkl	d_{obs}/nm	d_{calc}/nm	I/I_0
101	0.4754	0.4760	23
200	0.3609	0.3611	100
211	0.2876	0.2877	9
112	0.2688	0.2690	71
220	0.2552	0.2553	22
202	0.2379	0.2380	4
301	0.2248	0.2250	15
103	0.2024	0.2025	9
321	0.1909	0.1910	12
312	0.18516	0.18518	68
400	0.18050	0.18053	18
213	0.17663	0.17662	4
411	0.16883	0.16880	3
420	0.16146	0.16147	14
303	0.15866	0.15867	2
004	0.15821	0.15822	3
402	0.15679	0.15681	< 1
332	0.14988	0.14990	19
204	0.14493	0.14492	6
501, 431*	0.14079	0.14081	4
413, 224*	0.13646	0.13449	11
521	0.13119	0.13119	< 1
314	0.13008	0.13006	< 1
512	0.12929	0.12927	14
440	0.12768	0.12766	4
600	0.12036	0.12036	5
503, 433, 404*	1.18993	0.18992	8
215	0.11786	0.11785	3
611	0.11667	0.11668	1
532	0.11533	0.11533	13
620	0.11416	0.11418	6
523, 424*	0.11303	0.11301	14
541	0.11105	0.11103	< 1

*Greater peaks than the others in that series.

Table 2. Summary and Reliability Factors of Rietveld Refinement

Space group	$I4_1/amd$
Crystal system	Tetragonal
Z	4
No. of reflection	132
Lattice constants/nm	$a = 0.722134(1)$
	$b = 0.632896(1)$
Coordinates of O atom (16h)	
O_y	0.4326(5)
O_z	0.2053(7)
Theoretical density, D_x/g cm^{-3}	5.3927
Thermal parameters, B_{eq}/Å^2	
Eu(4a)	0.13(2)
Cr(4b)	0.55(4)
O(16h)	0.86(6)
R-factors	
R_{wp}	12.57
R_p	9.83
R_F	2.41
R_I	4.62
G of F	1.22

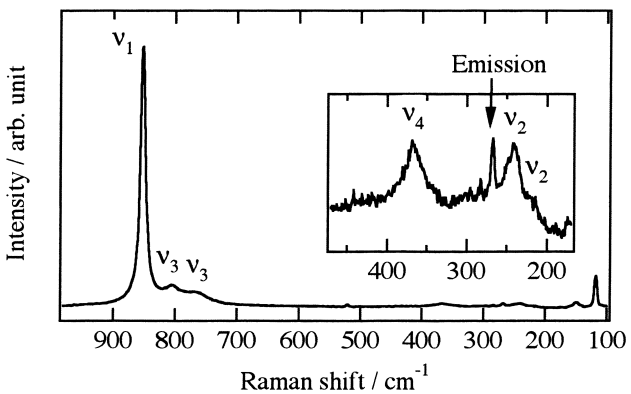

Fig. 2. Raman spectra for $EuCrO_4$. Insets are enlarged spectra of low intensity region.

1.3. The measured density of $EuCrO_4$ was 5.461 g cm^{-3}, which was about 1% larger than the calculated value in Table 2. The observed lattice constants are larger than those reported by Jiménes et al.,[5] but their Rietveld fitting was less accurate than ours: G of F factor calculated from R_{wp} and R_{exp} in their paper was 2.63, which exceeded the required limit. In addition, they did not measure the density to evaluate the fitting results. The atomic position of 16h oxygen was $y = 0.4326(1)$ and $z = 0.2053(1)$ and the bond lengths were 0.23468 nm for Eu–O and 0.17008 nm for Cr–O: the latter was only 0.06% shorter than that of $NdCrO_4$ (0.17018 nm).[6]

As reported previously,[6,7] all four vibrational modes of the CrO_4^{3-} tetrahedron, ν_1 (symmetric-stretching), ν_2 (symmetric-bending), ν_3 (antisymmetric-stretching), and ν_4 (antisymmetric-bending) are active to Raman spectroscopy. With $NdCrO_4$, these four bands appeared at $\nu_1 = 844.0$, $\nu_2 = 240.3$, $\nu_3 = 755.8$, and $\nu_4 = 363.9$, all in cm^{-1}, and no splitting of each mode was observed.[6] With $EuCrO_4$, however, ν_2 and ν_3 modes apparently split into two peaks, respectively, as shown in Fig. 2. There is a possibility for the triply degenerated ν_3 mode that it split into three peaks, and the third one was indistinguishable due to the strong ν_1 peak. The splitting can be attributed to the geometrical change of the CrO_4^{3-} tetrahedra. The symmetry of the tetrahedra is D_{2d} in both compounds, but the tetrahedron of $EuCrO_4$ is more elongated than that of $NdCrO_4$: O–O distances in the tetrahedron are 0.2845 nm and 0.2635 nm in $EuCrO_4$, whereas 0.2838 nm and 0.2639 nm in $NdCrO_4$. This difference is due to the smaller ionic radius of Eu(III) than Nd(III), since there is no substantial difference between the Cr–O bond lengths, as described above. Splitting of the degenerated ν_2 and ν_3 modes became more pronounced in $RECrO_4$ containing smaller RE(III) ions than Eu(III), as reported previously.[11] The two peaks below 150 cm^{-1} are lattice modes.

B. Mössbauer Spectra and Electronic Configurations. Narrow range Mössbauer spectra for $EuCrO_4$ measured at 15 K–room temperature are shown in Fig. 3, and a wide range spectrum at 15 K in Fig. 4. For all the materials investigated and at any temperature applied, the obtained ^{151}Eu Mössbauer spectra reflected the existence of Eu(III) without any detectable

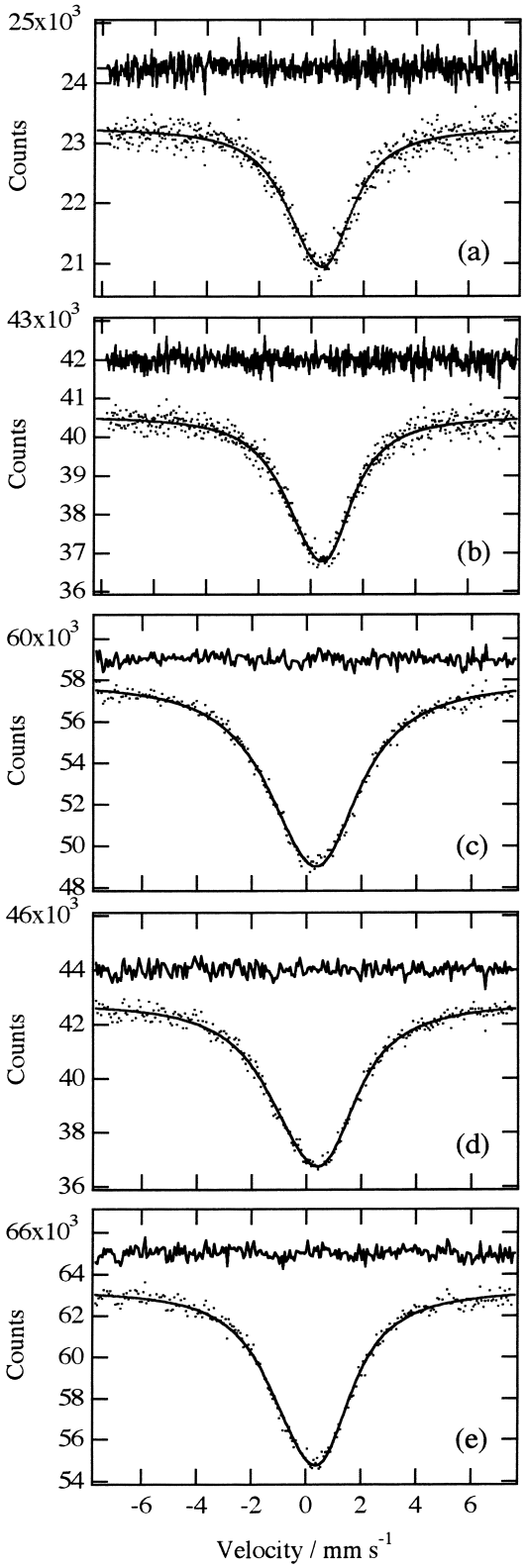

Fig. 3. Narrow range Mössbauer spectra for $EuCrO_4$ at (a) 15 K, (b) 30 K, (c) 77 K, (d) 195 K, and (e) room temperature.

contribution of Eu(II). As described above, $EuCrO_4$ and $EuVO_4$ belong to space group $I4_1/amd$, and the Eu site in these compounds has the point symmetry $\bar{4}m2$. This is axially symmetric, if no contribution to the electric field is present other than by surrounding ions. Then, the asymmetry parameter, η, is zero for $EuCrO_4$ and $EuVO_4$. The results of spectra analysis are summarized in Fig. 5. As the spectra at 15 K and 30 K for $EuCrO_4$ were measured with a different equipment and geometry, the amplitude, base line, and line width cannot be compared with the results at other temperatures.

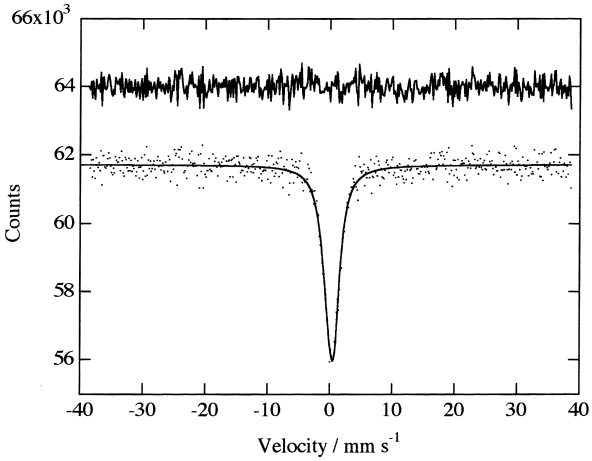

Fig. 4. Wide range Mössbauer spectrum for $EuCrO_4$ at 15 K.

The spectra displayed a small unresolved quadrupole splitting, showing that there is a finite electric field gradient at the location of the ^{151}Eu nucleus. The main component of the electric field gradient, V_{zz}, for $EuCrO_4$ was positive, and did not show any appreciable temperature dependence, as shown in Fig. 5a. The V_{zz} for $EuVO_4$ at room temperature was similar to that of $EuCrO_4$. Normally, the value of V_{zz} should increase, since the structure shrinks (Eu–O distance decreases) with lowering temperature. The result, however, was not like that. This structurally insensitive behavior might be attributed to the strong ionic character of Eu(III) in it, as described below. The absolute value of V_{zz} for $EuCrO_3$ increased very slightly with temperature, though the sign of V_{zz} was opposite (negative). The η for $EuCrO_3$ were 0.5–0.8, reflecting the existence of an electric field gradient whose symmetry is lower than axial at the location of the ^{151}Eu nucleus.

The ^{151}Eu isomer shift, IS, for both $EuCrO_4$ and $EuCrO_3$ slightly increased with decreasing temperature, as shown in Fig. 5b, which was the expected tendency considering the second order Doppler shift. The IS at room temperature increased in the order of $EuVO_4$ (0.19 mm s^{-1}) < $EuCrO_4$ (0.21 mm s^{-1}) < $EuCrO_3$ (0.74 mm s^{-1}), but was smaller than that for Eu_2O_3 (0.85 mm s^{-1} [16]). The IS for $EuCrO_4$ is comparable to that for Eu–malonate complex ($Eu_2(CH_2C_2O_4)_3 \cdot 5H_2O$, 0.17 mm s^{-1} [16]) but smaller than that of Eu–oxalate complex ($Eu_2(C_2O_4)_3 \cdot 10H_2O$, 0.31 mm s^{-1} [16]). In the ionic compound EuF_3, the electronic configuration of Eu is expected to be $4f^6 6s^x$, where x is close to zero and Eu_2O_3 has some covalent nature in bonding (probably 20–25%). As the isomer shift is a kind of measure for the electron density around the nucleus, the population of electrons in the 6s orbital is lowest in EuF_3 and highest in Eu_2O_3. The other three compounds are in between them. The IS indicates that the electron density of 6s orbital in $EuCrO_4$ is very low, suggesting that Eu^{3+} and CrO_4^{3-}

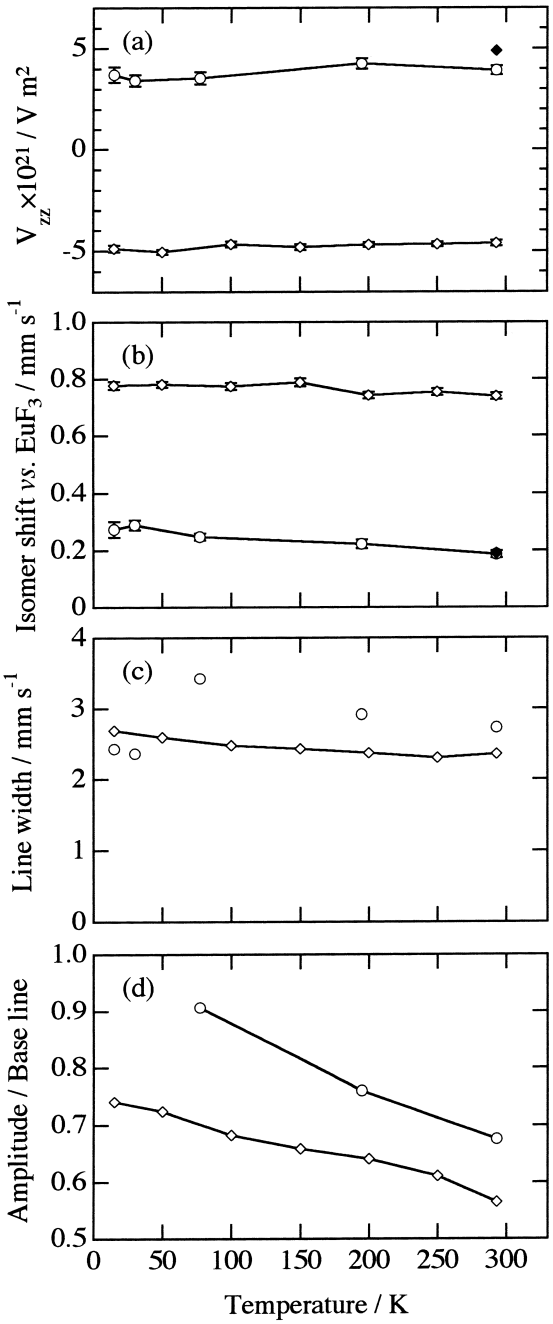

Fig. 5. Temperature dependence of Mössbauer parameters for $EuCrO_4$ (○) and $EuCrO_3$ (◇): (a) the main component of the electric field gradient, V_{zz}, (b) isomer shift vs EuF_3, (c) line width, and (d) Area/Baseline function representing Mössbauer–Lamb factor. The data for $EuVO_4$ (◆) are also shown in (a) and (b). Error bars are $\pm 1\sigma$.

are polarized similarly to $EuVO_4$: both have the same zircon type structure and coordination number for Eu.

The magnetic splitting was not observed for both $EuCrO_4$ and $EuCrO_3$, but the line width increased with lowering temperature for the same run of measurements. For $EuCrO_4$ in Fig. 5c, it increases from room temperature to 77 K and from 30 K to 15 K: each set was measured differently, as described above.

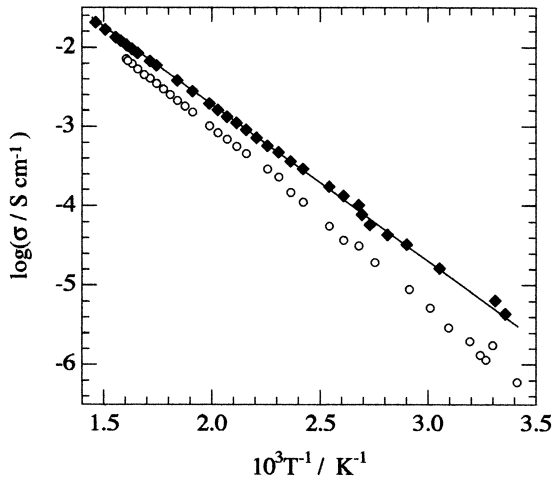

Fig. 6. Arrhenius plot of the electric conductivity of $EuCrO_4$ (◆) at 300–670 K. Conductivity for $NdCrO_4$ is shown by ○ for comparison.

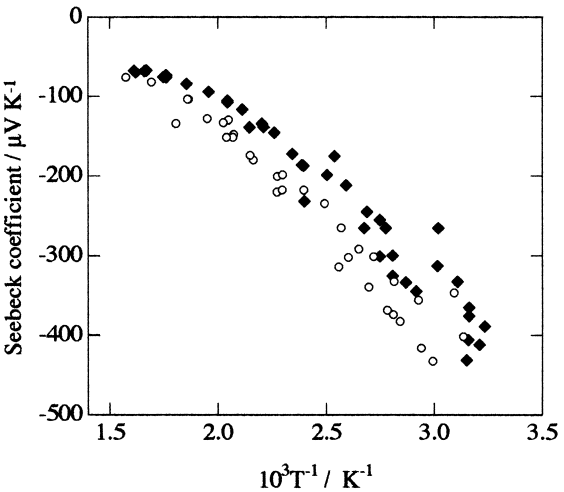

Fig. 7. Seebeck coefficient of $EuCrO_4$ (◆) as a function of the reciprocal temperature (300–670 K). The Seebeck coefficient for $NdCrO_4$ is shown by ○ for comparison.

The temperature dependence of the Mössbauer-Lamb factor is represented by the temperature dependence of the $\log_e$(Area/Baseline) function (Fig. 5d). For both $EuCrO_4$ and $EuCrO_3$, it decreased with increasing temperature as expected. Assuming the validity of the Debye model for $EuCrO_4$, we can obtain a Debye temperature of $\Theta_D = 338 \pm 10$ K. This value is only slightly lower than 354 ± 20 K found for $EuCrO_3$, which reflects that the vibrational state of Eu is similar in the two compounds.

C. Electric and Magnetic Properties. The apparent electric conductivity and Seebeck coefficient of $EuCrO_4$ are plotted against the reciprocal temperature (300–670 K), as shown in Figs. 6 and 7, where data for $NdCrO_4$[8] are also plotted for comparison. The apparent activation energy was 38 kJ mol^{-1}, and slightly smaller than those of $LaCrO_4$ and $NdCrO_4$. The electric conductivity was the highest of the three, but still lower than that of the mixed valence compounds $Nd_{1-x}Ca_xCrO_4$ ($x = 0.1$, 0.2). As reported previously, the electric

conduction is not attributed to protons or other ionic species.[8] These results clearly indicate that both compounds are semiconductors, and that the carrier is mainly electrons because of the negative values of the Seebeck coefficient. There is no reason that the conduction mechanism of $EuCrO_4$ is different from that of $NdCrO_4$.[8] The mechanism is explained in the same way by a band scheme. The bands are formed due to an intermixing of ligand-to-metal charge-transfer (LMCT) state into the ionic configuration:[9,10] the top of the valence band mainly consists of Cr $d\pi^*$ states and the bottom of the conduction band O $p\sigma^*$ states. Therefore, electric conduction takes place by excitation of the unpaired electrons on Cr $d\pi^*$ states into the conduction band of $p\sigma^*$ states. The result of Mössbauer spectroscopy that Eu(III) in $EuCrO_4$ is strongly ionic also supports this mechanism, that is, electronic conduction occurs between the CrO_4^{3-} tetrahedra.[8] This anomalous conduction is attributed to the unusual valence state of Cr(V) which causes an intermixing of the LMCT state, since normally monazite- and zircon type oxides, for example $REMO_4$ (RE: trivalent rare earth, M: V, P, As, etc.), are insulators.[17,18] This type of conduction has been reported for other high valence state oxides.[9]

The temperature dependence of the molar susceptibility, χ, is shown in Fig. 8. The curve shape resembles that reported by Jiménes et al.,[5] but the χ, is smaller by 10–20% than their data at all the temperatures measured. The data in Fig. 8 are not corrected for ionic diamagnetism but this cannot be a reason for the difference, as the magnitude of correction is about 6×10^{-5} emu mol^{-1}. There is a possibility that it originated from the purity of the sample and measurements. The value of χ^{-1} followed the Curie–Weiss' law down to about 130 K but not below that. From the slope of this part, the total magnetic moment, μ_{tot}°, was calculated to be 1.54 μ_B (μ_B is a Bohr magneton). This value is smaller than the theoretical one for Cr(V) ($\mu_{Cr}^{t} = 1.72\ \mu_B$),[8] indicating no contribution of Eu(III) to the magnetic moment of $EuCrO_4$. Since the Curie–Weiss' law was established only for a limited temperature range, further discussion is not appropriate. Some magnetic transitions are observed around 15 K (Fig. 8, inset). This cannot be distinguished from the Mössbauer spectra at 15 K (Figs. 3a and 4),

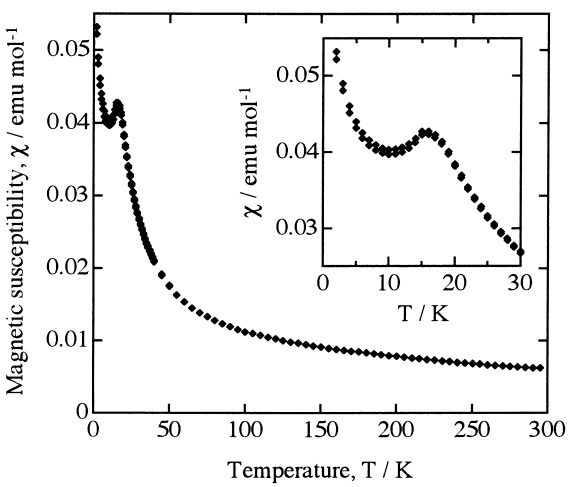

Fig. 8. Temperature dependence of magnetic susceptibility for $EuCrO_4$. The inset shows the change at 0–30 K.

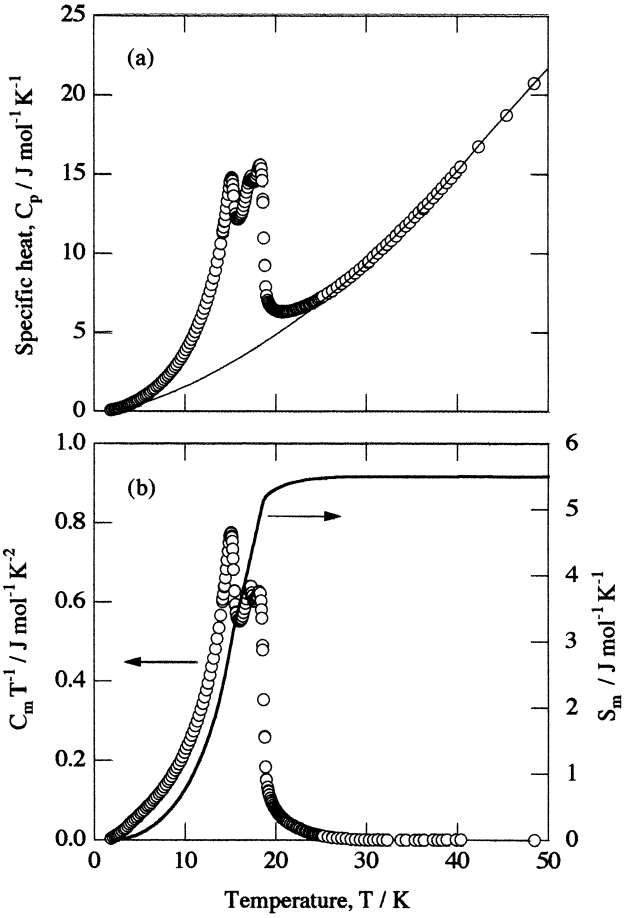

Fig. 9. Temperature dependence of (a) specific heat, C_p, and (b) magnetic specific heat, C_m, for $EuCrO_4$. The magnetic contribution of the entropy, S_m, is also shown in (b).

since the transitions are not completed at this temperature and the spectrum below this was not available.

To examine the details of the magnetic transition and to estimate the energy levels involved in the process of magnetic ordering, specific heat, C_p, was measured in a low temperature region. There were three anomalies at 15.1, 17.2 and 18.2 K, as shown in Fig. 9a. A separation of the magnetic specific heat, C_m, was carried out by assuming that the contribution of C_m to C_p is negligible above 30 K. The C_p values between 30 and 50 K were extrapolated using a virial expansion as Fig. 9a, and all contributions other than C_m were subtracted. The value C_m/T is plotted on the left axis against the temperature and the magnetic entropy (the integral of C_m/T), S_m, on the right in Fig. 9b. The S_m was 5.54 J mol^{-1} K^{-1} and very close to $R \log_e 2$ (= 5.76 J mol^{-1} K^{-1}), indicating that only two states are involved in the process. This suggests that the magnetic entropy is due to Cr(V), which has a spin quantum number of $s = 1/2$, indicating that the observed anomalies result from the antiferromagnetic transition of Cr(V). However, no simple explanation for the three anomalies observed in Fig. 9 can be offered at the present time.

Summary

Single phase zircon type $EuCrO_4$ (S.G. $I4_1/amd$) was synthesized by the pyrolysis of the precursor prepared from an

equimolar mixture of $Eu(CH_3COO)_3 \cdot 4H_2O$ and CrO_3, and the structure including atomic positions was precisely determined by X-ray Rietveld refinement. The electronic and magnetic properties of the compound were studied by (1) electric conductivity and Seebeck coefficient measurements at 300–670 K, (2) Raman spectroscopy, (3) Mössbauer spectroscopy at 15 K–room temperature, and (4) magnetic susceptibility and specific heat measurements at 2–300 K. The CrO_4^{3-} tetrahedra (symmetry: D_{2d}) in $EuCrO_4$ were slightly elongated compared with that in $NdCrO_4$ due to the smaller ionic radius of Eu(III) than Nd(III), which caused a splitting of the degenerated vibration modes of CrO_4^{3-}, ν_2 and ν_3, in Raman spectra. The ^{151}Eu Mössbauer spectra showed not a trace of the Eu(II) species in the compounds measured in the present work. The Debye temperature, Θ_D, estimated from the Mössbauer spectra suggested that the vibrational state of Eu(III) in $EuCrO_4$ was similar to that in the perovskite type $EuCrO_3$. However, the isomer shift of the Mössbauer spectra revealed that the electron density of the 6s orbital of Eu(III) in $EuCrO_4$ was very low and almost the same with that in the zircon type $EuVO_4$, that is, Eu(III) in these compounds has highly ionic character, whereas the electron density of the 6s orbital of Eu(III) in $EuCrO_3$ was higher and nearly the same with the one in Eu_2O_3. The $EuCrO_4$ was found to be an *n*-type semiconductor similar to $NdCrO_4$, while zircon type $REMO_4$ (M: V, P, As, etc.) are insulators. The electric conductivity of $EuCrO_4$ was better than those of $LaCrO_4$ and $NdCrO_4$, and the apparent activation energy was 38 kJ mol^{-1} which was slightly smaller than those of $LaCrO_4$ and $NdCrO_4$. Magnetic susceptibility and specific heat measurements showed that the antiferromagnetic transition took place at around 15 K, and was solely due to Cr(V) from the magnetic entropy value of 5.54 J mol^{-1} K^{-1}.

References

1 H. Walter, H. G. Kahle, K. Mulder, H. C. Schopper, and H. Schwarz, *Int. J. Magn.*, **5**, 129 (1973).

2 G. Buisson, F. Tcheou, F. Sayetat, and K. Scheuemann, *Solid State Commun.*, **18**, 871 (1976).

3 M. Steiner, H. Dachs, and H. Ott, *Solid State Commun.*, **29**, 231 (1979).

4 A. Morales-Sanchez, F. Fernandez, and R. Saez-Puche, *J. Alloy. Comp.*, **201**, 161 (1993).

5 E. Jiménez, J. Isasi, and R. Saez-Puche, *J. Alloy. Comp.*, **312**, 53 (2000).

6 Y. Aoki, H. Konno, H. Tachikawa, and M. Inagaki, *Bull. Chem. Soc. Jpn.*, **73**, 1197 (2000).

7 Y. Aoki and H. Konno, *J. Solid State. Chem.*, **156**, 370 (2001).

8 Y. Aoki, H. Konno, and H. Tachikawa, *J. Mater. Chem.*, **11**, 1214 (2001).

9 M. Atansov, H. Adamsky, and K. Eifert, *J. Solid State Chem.*, **128**, 1 (1997).

10 M. Atansov, *Z. Physik. Chem.*, **200**, 57 (1997).

11 Y. Aoki and H. Konno, *J. Mater. Chem.*, **11**, 1458 (2001).

12 Z. Klencsár, E. Kuzmann, and A. Vértes, *J. Radioanal. Nucl. Chem.*, **210**, 105 (1996).

13 J. Lindén, J. Hietaniemi, E. Ikonen, M. Lippmaa, I. Tittonen, T. Katila, T. Karlemo, M. Karppinen, L. Niinistö, and K. Ullakko, *Phys. Rev.*, **B 46**, 8534 (1992).

14 H. Schwarz, *Z. anorg. allge. Chem.*, **323**, 275 (1963).

15 B. C. Chakoumakos, M. M. Abraham, and L. A. Boatner, *J. Solid State Chem.*, **109**, 197 (1994).

16 P. Glentworth, A. L. Nicols, D. A. Newton, N. R. Large, and R. J. Bullock, *J. Chem. Soc., Dalton Trans.*, **1973**, 546.

17 K. Gaur and H. B. Lal, *J. Mat. Sci.*, **19**, 3325 (1984).

18 K. Gaur and H. B. Lal, *J. Mat. Sci.*, **20**, 3167 (1985).